Molecular BioSystems

Accepted Manuscript

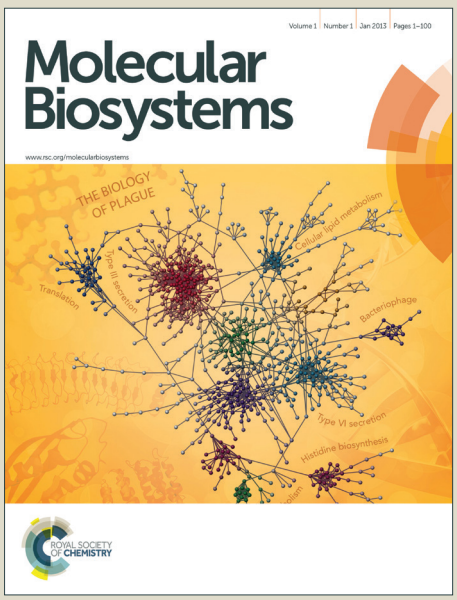

This is an *Accepted Manuscript*, which has been through the Royal Society of Chemistry peer review process and has been accepted for publication.

Accepted Manuscripts are published online shortly after acceptance, before technical editing, formatting and proof reading. Using this free service, authors can make their results available to the community, in citable form, before we publish the edited article. We will replace this *Accepted Manuscript* with the edited and formatted *Advance Article* as soon as it is available.

You can find more information about *Accepted Manuscripts* in the Information for Authors.

Please note that technical editing may introduce minor changes to the text and/or graphics, which may alter content. The journal's standard Terms & Conditions and the Ethical guidelines still apply. In no event shall the Royal Society of Chemistry be held responsible for any errors or omissions in this *Accepted Manuscript* or any consequences arising from the use of any information it contains.

ROYAL SOCIETY OF CHEMISTRY

www.rsc.org/molecularbiosystems

A time resolved metabolomics study: The influence of different carbon sources during growth and starvation of *Bacillus subtilis*

Hanna Meyer[1], Hendrikje Weidmann[2,3], Ulrike Mäder[2], Michael Hecker[4], Uwe Völker[2], Michael Lalk[1¶]

[1]Institute of Biochemistry, Felix-Hausdorff-Strasse 4, 17487 Greifswald, Ernst-Moritz-Arndt-University Greifswald, Germany

[2]Interfaculty Institute of Genetics and Functional Genomics, Department of Functional Genomics, Friedrich-Ludwig-Jahn-Str. 15a, 17475 Greifswald, University Medicine Greifswald, Germany

[3]current address: Oncotest GmbH, Am Flughafen 12-14, 79108 Freiburg

[4]Institute for Microbiology, Friedrich-Ludwig-Jahn-Str. 15, 17475 Greifswald University of Greifswald, Greifswald, Germany

Category: Full research article

[¶]Corresponding address:

Institute of Biochemistry, Felix-Hausdorff-Strasse 4, 17487 Greifswald, Ernst-Moritz-Arndt-University Greifswald, Germany

Phone: +49 3834 864867, Fax: +49 3834 864413

Email: lalk@uni-greifswald.de

Molecular BioSystems Accepted Manuscript

Keywords: *Bacillus subtilis*, central carbon metabolism, carbon source, adaptation, overflow metabolism, targeted metabolomics, quantitative metabolomics, adenylate energy charge, metabolite equilibrium.

Abstract:

In its natural environment the soil, the Gram-positive model bacterium *Bacillus subtilis* frequently encounters nutrient limitation and other stress factors. Efficient adaptation mechanisms are necessary to cope with this wide range of environmental challenges. The ability to utilize diverse carbon sources represents a key adaptation process that allows *B. subtilis* to thrive in its natural habitat.

To gain a comprehensive insight into the metabolism of *B. subtilis,* global metabolite analyses were performed during growth with glucose alone or glucose with either malate, fumarate or citrate as carbon/energy sources. Furthermore, to achieve comprehensive coverage of a wide range of chemical different metabolites, complementary GC-MS, LC-MS and ^{1}H-NMR analyses were applied.

This study reveals that the availability of different carbon sources results in different extracellular metabolite profiles whereas a regulated intracellular metabolite equilibrium was observed. In addition, the typical energy-starvation induced activation of the general stress sigma factor σ^{B} was only observed upon entry into stationary phase with glucose or glucose and malate as carbon sources.

Introduction:

Besides *Escherichia coli, Bacillus subtilis* constitutes the most thoroughly investigated bacterium. Moreover, *B. subtilis* and its close relatives are important for biotechnology and frequently used for the overproduction of enzymes[1], and primary as well as secondary metabolites[2] including antibiotics[3,4]. The synthesis and secretion of the latter products are primarily observed under growth-limiting conditions. Hence, studies characterizing the transition from an exponentially growing to a non-growing state not only provide a deeper insight into the physiology of *B. subtilis* but also have

Molecular BioSystems Accepted Manuscript

the potential to contribute to optimization of industrial fermentation conditions[5]. In its natural habitat *B. subtilis* has to cope with a number of stress factors and limitation/starvation conditions. Accordingly, adaptation responses to a wide range of environmental stresses and nutrient limitation situations have been thoroughly investigated[6-10].

Adjustments of gene expression are a prime mechanism through which the cells adapt to changing environments. As a consequence thereof, the biosynthesis of a number of proteins is up or down regulated. Besides metabolic enzymes this adaptation also involves control of activity of regulatory proteins such as the alternative sigma factor σ^B [11].

Building on this knowledge, this work aims to extend the understanding of these processes by studying the direct physiological consequences of the adaptation using metabolomics. We focus on adaption to different carbon sources because limitation of carbon and energy sources is a prime growth limiting factor in soil[12]. Besides glucose, the preferred carbon source of *B. subtilis*, a wide range of other carbon/energy sources are available in the natural environment of *B. subtilis.* These are produced and secreted by different plants, fungi and lichens or become available for bacteria upon decomposition of plant material. Since intermediates of the tricarboxylic acid cycle (TCA cycle) such as fumarate, malate and citrate are also available in soil[12], we tested the influence of the addition of them to glucose minimal medium onto the extra- and intracellular metabolite profile of growing and starving *B. subtilis* cells. Using a combination of complementary ^{1}H-NMR, LC-MS and GC-MS analyses, our approach aims to unravel how the previously analyzed changes on transcriptome and proteome level[5, 13] trigger adaptations in the metabolome of *B. subtilis*. Since the metabolic profile of a cell reflects the final state of the adaptation process, the ability of *B. subtilis* to maintain an equilibrium on the metabolomic level, a property which was previously reported for *Pseudomonas putida* by van der Werf and colleagues[14], was analysed in detail. Compared to changes in gene expression and protein composition, the metabolite profile is a more direct indication for the cellular adaptation. Indeed, data of the intracellular metabolome confirm the hypothesis of an intracellular metabolite equilibrium, since pools of intracellular metabolites were largely maintained independent of the carbon source composition. Even between exponential and stationary growth phase only

Molecular BioSystems Accepted Manuscript

specific differences were observed, while the overall metabolite pool was very similar. Despite the intracellular metabolite equilibrium, rather extensive changes in the exo-metabolome were observable depending on the carbon sources available. Additionally, contrary to the rather stable intracellular metabolite pool, carbon source dependent differences in the activation of the alternative RNA polymerase sigma factor σ^B were observed when cells entered the stationary phase.

Results and discussion:

In this study, for the analyses of the extracellular and intracellular metabolome complementary GC-MS, LC-MS and ^{1}H-NMR analyses were applied.

^{1}H-NMR analyses were performed to investigate the extracellular metabolome. This includes the utilization of carbon sources, the accumulation of small molecules in the growth medium and the overflow metabolism of *B. subtilis*.

Moreover, numerous intracellular metabolites were identified and quantified using GC-MS (EI/quadrupol) and LC-MS (ESI/time of flight) measurements.

Growth and carbon source utilization

Glucose is considered to be the preferred carbon source of *B. subtilis*[15-18] and thus we wanted to investigate, if additional alternative carbon sources are subject to glucose dependent carbon catabolite repression (CCR). For this purpose, *B. subtilis* was grown with glucose as the only carbon source (0.1% ≙ 5.55 mM) or a combination of glucose and similar amounts of a second carbon source (0.1 % malate, citrate or fumarate). Surprisingly, *B. subtilis* displayed quite some cell lysis when cells entered the stationary phase as a result of the exhaustion of glucose, preventing any type of quantitative systems-type of analysis. Thus, we also wanted to assess if this lysis could be reduced or even prevented by inclusion of additional carbon sources in the medium.

Irrespective of the additional carbon source added, exhaustion of glucose triggered entry into stationary phase (Figure 1). Glucose utilization itself differed slightly between the four investigated cultivation conditions. When malate or fumarate was available in addition to glucose, glucose was

Molecular BioSystems Accepted Manuscript

utilized faster compared to growth with glucose as the sole carbon source. In contrast, addition of citrate to the medium resulted in slightly slower glucose utilization compared to growth on glucose as the sole carbon source. Moreover the growth rate varied and was highest for glucose and malate (Figure 1).

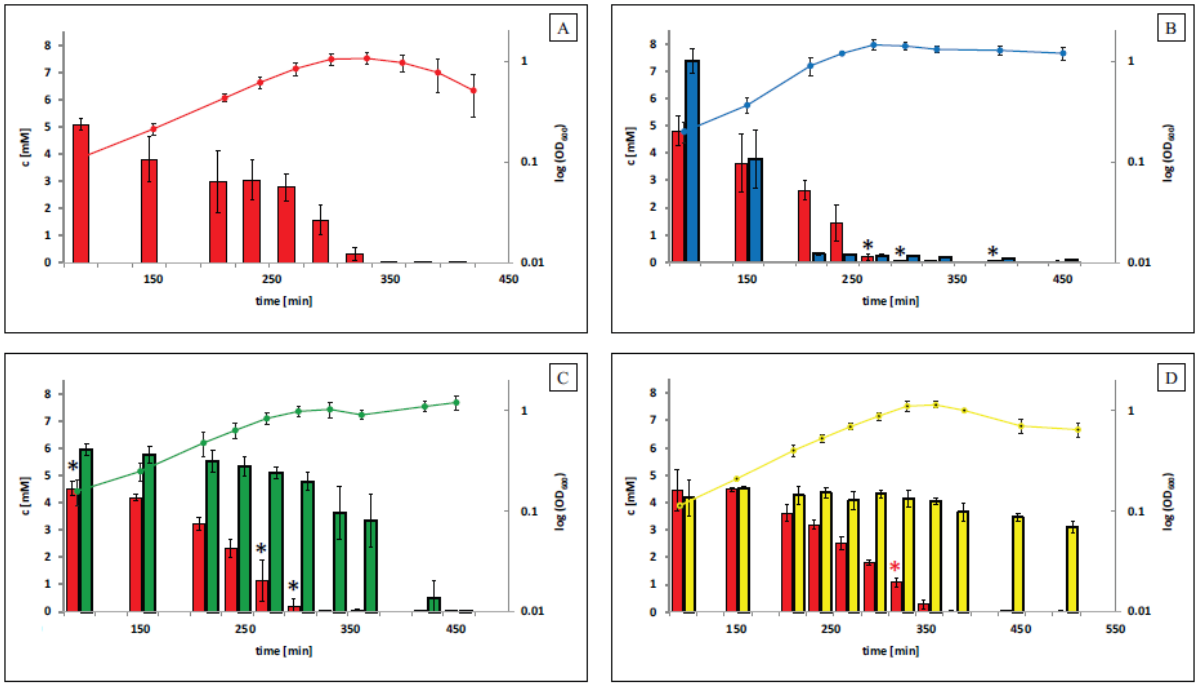

Figure 1: Growth and carbon source utilization of *B. subtilis* during growth with A) only glucose, B) glucose and malate, C) glucose and fumarate and D) glucose and citrate. The lines illustrate the growth measured as optical density (OD) and the bars show the utilization of the carbon source(s).

Black stars indicate significant (p-value ≤ 0.05) lower glucose concentration compared to growth with only glucose as carbon source and red stars indicate significant (p-value ≤ 0.05) higher glucose concentration compared to the only glucose condition.

During cultivation with glucose and malate, both carbon sources were utilized in parallel. Probably this co-metabolization of malate with glucose and/or the faster glucose utilization causes the higher growth rate during growth on glucose and malate. The observation, that malate was co-metabolized with glucose is in agreement with previous reports ([18, 19]), showing that malate utilization is not subject to glucose dependent CCR. Besides, it was noticed that malate consumption was faster than

Molecular BioSystems Accepted Manuscript

that of glucose. As intended, during growth on glucose and malate as carbon sources the optical density remained constant after entry into stationary phase and no cell lysis was observed.

Diauxic growth was observed during growth on glucose and fumarate. Fumarate utilization was initiated after 270 min of growth, where still approximately 1 mM glucose was available. Nevertheless, the main fumarate utilization started only after glucose was exhausted, indicating that fumarate was subject to glucose dependent CCR in *B. subtilis*.

During growth on glucose and citrate no diauxic growth was detected. Consumption of citrate was not initiated before glucose was exhausted (after 360 min). This indicates, that also citrate was subject to glucose dependent CCR in *B. subtilis*. Contrary to fumarate, citrate was utilized to only a minor extent after the exhaustion of glucose and was not completely consumed during the timeframe of the experiment (Figure 1).

Overflow metabolism

Beside differences in carbon source utilization, several differences were revealed in the overflow metabolome. Overflow metabolism is a typical phenomenon found in bacteria if the substrate uptake and therewith the rate of glycolysis exceeds a critical value. This is mostly associated with the secretion of compounds like acetate, acetoin and 2,3-butanediol.

Under all conditions investigated, the most abundant overflow metabolite was acetate and highest acetate overflow occurred when *B. subtilis* was grown with glucose and malate as carbon sources (Figure 2). When cells entered stationary phase (270 min) due to glucose starvation, the acetate concentration in the medium remained constant. Consistent with this finding, it was reported previously that transcript and protein levels of the acetate kinase (AckA) decreased during stationary phase[5]. The constant acetate concentration in stationary growth phase implies that acetate was not reutilized as an alternative carbon source by *B. subtilis* under the conditions investigated. This failure to reutilize acetate was likely caused by the absence of genes necessary for the glyoxylate cycle in *B. subtilis.*

Molecular BioSystems Accepted Manuscript

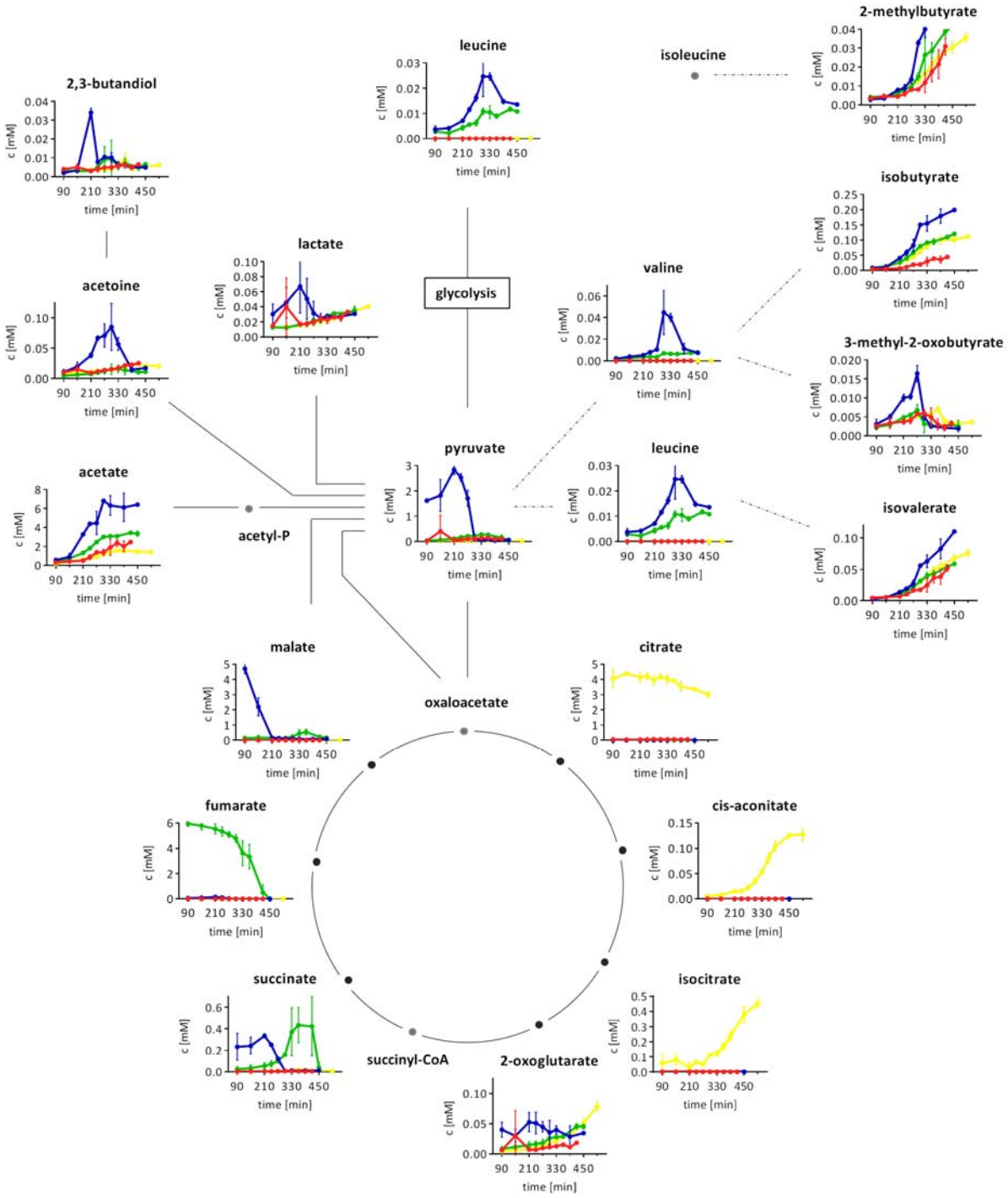

126

127 ***Figure 2**:* Time resolved extracellular metabolite concentration (c [mM]) for red: only glucose, blue:

128 glucose and malate, green: glucose and fumarate and yellow: glucose and citrate. The y-axis scaling is

129 different between the plotted metabolites, corresponding to the respective concentration range.

130 Since malate was available in the growth medium, the y-axis for malate ranges from 0 mM to 5 mM.

131

Molecular BioSystems Accepted Manuscript

Moreover, if both glucose and malate were supplied as carbon sources high levels of pyruvate were already secreted during exponential growth as already shown by Kleijn and colleagues[18] (Figure 2). Extracellular pyruvate levels amounted up to approximately 25 % of the initial amount of malate supplied. Increased pyruvate secretion might have been due to increased generation of pyruvate and NAD(P)H[20] via the oxidative decarboxylation of malate and the excess pyruvate was secreted. In the presence of malate[21] transcription of the genes encoding the malic enzyme (four putative paralogs: *maeA, malS, mleA* and *ytsJ*[20]) is activated by the MalK-MalR (formerly YufL/YufM) two-component system, which also regulates expression of the malate transporters MaeN (formerly YufR) and YflS. After 210 min of growth, malate was consumed and subsequently pyruvate reutilization started and extracellular pyruvate levels collapsed, even though small amounts of glucose (1.43 ± 0.67 mM) still were available (Figure 1 and 2).

Besides the replenishment of the TCA cycle via the NAD-dependent pyruvate dehydrogenase complex (PdhA/B/C/D), via the NADP-dependent malic enzyme (YtsJ), or via the pyruvate carboxylase (PycA) pyruvate can be converted to acetoin via the acetolactate synthase (AlsS) and the acetolactate decarboxylase (AlsD). The extracellular acetoin concentration was significantly (p-value ≤ 0.05) higher during cultivation with glucose and malate as carbon sources compared to cultivation on glucose only (Figure 2). This supports the notion that expression of *alsS* and *alsD*, which are required for acetoin formation, was induced in the presence of organic acids as postulated by Schilling and co-workers[22]. These authors observed that the *alsSD* operon was strongly induced by the presence of glutamate and succinate and concluded that the *alsSD* operon is induced by organic acids, even though they observed no acetoin accumulation in the medium under either condition[22]. Likewise, in the current study, acetoin did not accumulate when *B. subtilis* cells were cultivated with glucose and fumarate or glucose and citrate as carbon sources. Supporting the notion of Schilling and colleagues[22] we suggest that not pH changes but rather acetate accumulation constituted a potential stimulus for acetoin formation, since the pH remained constant during growth (supplementary data 1). This hypothesis gains support by the observation of significantly (p-value ≤ 0.05) higher acetate, and acetoin accumulation in the medium during exponential growth with glucose and malate as carbon

Molecular BioSystems Accepted Manuscript

source mixture. However, in our experimental setup the acetoin concentration decreased during stationary phase, whereas the extracellular acetate concentration remained continuously high. On the other hand acetoin and pyruvate concentration decreased concomitantly during growth on glucose and malate. Hence, pyruvate, which is precursor of acetoin, could be an alternative stimulus of acetoin formation.

Acetoin can be reduced to 2,3-butanediol via the BdhA (acetoine/ butanediol dehydrogenase) in order to regenerate $NAD(P)^+$. As for acetoin, higher amounts of 2,3-butanediol were detected after 210 min of growth in the presence of glucose and malate as carbon sources. Although the acetoin concentration decreased in stationary phase, no increased 2,3-butanediol accumulation was observed (Figure 2). In the stationary growth phase the TCA is active and facilitates the regeneration of NAD^+. Hence, the absence of 2,3-butanediol production might be due to dispensable $NAD(P)^+$ regeneration via BdhA. Instead of conversion of acetoin to 2,3-butanediol, the data presented here indicate that acetoin is reutilized[23,24]. This is in agreement with the observation that transcription of the acetoin dehydrogenase (*acuA/B/C*)[25] and the acetoin dehydrogenase (*acoA/B/C*, E1 and E2 component)[26] were repressed in the presence of glucose (CcpA dependent), and that their expression was induced when glucose is exhausted and cells entered the stationary growth phase[25].

Extracellular TCA cycle intermediates

As different TCA cycle intermediates were available as carbon sources, possible differences in the extracellular levels of these metabolites were also investigated.

Indeed, isocitrate and cis-aconitic acid accumulation in the growth medium were only observed during growth on glucose and citrate. Concentrations of both metabolites increased 10 fold from exponential to stationary growth phase. Although the levels of both compounds compared to citrate levels in the medium are rather low (isocitrate: 8.7 % and cis-aconitate: 2.6 %), during the time window between 360 min – 510 min, the secreted amounts of isocitrate and cis-aconitate constituted approximately 30 % and 5.5 %, respectively, of the citrate consumed.

Molecular BioSystems Accepted Manuscript

Using the combination of glucose and fumarate as carbon source mixture, succinate accumulated in significantly higher concentrations (p-value ≤ 0.05; up to 0.45 mM) compared to growth on glucose or glucose and citrate during stationary phase. Notably succinate secretion was initiated simultaneously with fumarate consumption. Succinate levels in the medium dropped when fumarate was exhausted (at 450 min). Moreover, malate was secreted up to 0.55 mM in the stationary phase with glucose and fumarate as carbon sources. This malate overflow was observed to start simultaneously with fumarate utilization during the transition from exponential to stationary growth phase. As for succinate, the extracellular malate level then declined with fumarate limitation (Figure 2).

Increased extracellular succinate levels were moreover observed in the exponential growth phase in the glucose and malate cultures. Under these specific circumstances, succinate reutilization started even though approximately 2.6 mM of glucose were still available but malate was exhausted. This indicates a co-utilization of glucose and succinate, which was secreted by *B. subtilis* during malate excess (Figure 2).

Uncommon overflow metabolism

In addition to the common overflow metabolism and the secretion of TCA cycle intermediates, an accumulation of valine and leucine, as well as intermediates of the branched chain amino acid (BCAA) and branched chain fatty acids (BCFA) metabolism, in the medium were detected (Figure 2). Both valine and leucine, which are synthesized from pyruvate, were only secreted when cells were grown on glucose and malate or glucose and fumarate and reached a maximal extracellular concentration during glucose and malate cultivation. This seems reasonable because secreted amounts of the precursor pyruvate were also significantly higher during glucose and malate cultivation (p-value ≤ 0.05). Levels of valine and leucine were 10 fold higher in glucose and malate medium compared to growth on glucose as the only carbon source (Figure 2). On the other hand, isoleucine, the synthesis of which requires both pyruvate and threonine[27] did not accumulate.

Molecular BioSystems Accepted Manuscript

While pyruvate and succinate reutilization started at 210 min, when malate was exhausted, reutilization of valine, leucine and 2-methyl-2-oxobutyrate did not initiate before glucose was exhausted (270 min, Figure 2).

Extracellular concentrations of isobutyrate, isovalerate and 2-methylbutyrate increased steady during growth under all conditions (Figure 2).

Summary overflow metabolism

Summarizing, access of malate, which is co-metabolized with glucose triggers increased accumulation of pyruvate, acetoine and succinate during exponential growth. These were immediately metabolized once malate was consumed. During growth with glucose and malate as mixed carbon sources, the highest extracellular metabolite amounts were measured. We speculate that the stronger metabolite accumulation during cultivation on glucose and malate is related to a higher influx of carbon-sources since malate and glucose were utilized in parallel. This likely caused strong conversion of malate to pyruvate and a conversion of surplus pyruvate to other overflow metabolites derived from pyruvate. As soon as malate was exhausted, pyruvate re-consumption started, indicating that pyruvate was used as carbon-source. Finally, after pyruvate was exhausted, the extracellular concentrations of acetoin, leucine and valine decreased, probably due to the usage of these metabolites as alternative carbon sources.

Intracellular metabolome

Complementing the analysis of the extracellular metabolome we also assessed whether similar differences exist in the intracellular metabolome, or whether an intracellular metabolite equilibrium was maintained independently of the carbon source supply.

The principal component analysis (PCA) in figure 3 indicates that the intracellular metabolome between the four growth conditions was significantly more stable than the exo-metabolome. The extracellular metabolite samples clustered carbon source dependent (second carbon source was excluded for PCA analysis) as well as growth phase dependent. Thus, an obvious carbon source

Molecular BioSystems Accepted Manuscript

238 and/or growth phase dependent clustering is not detectable in the PCA of the intracellular
239 metabolite samples (Figure 3). This is a first evidence for a robustness of the pools of intracellular
240 metabolites.

241

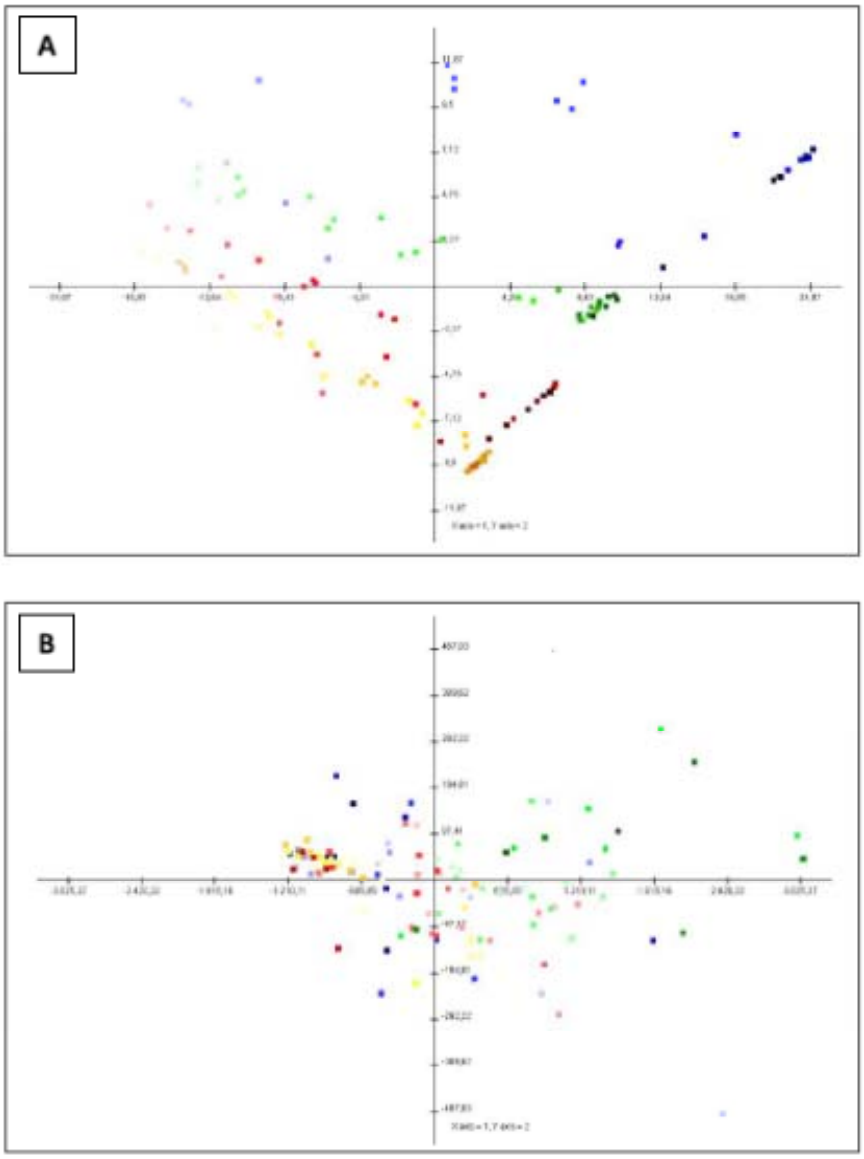

242

243 ***Figure 3***: Principal component analysis

244 The principal component analysis (PCA) was performed by tMev using the mean centering
245 mode.

246 A) PCA based on all quantified extracellular metabolites (exclusive malate, fumarate and
247 citrate) for all sampling time points with following PC variances; PC1: 68.89 %, PC2: 18.19 %.

Molecular BioSystems Accepted Manuscript

B) PCA based on all quantified intracellular metabolites for all sampling time points with following PC variances; PC1: 95.75%, PC2: 1.27 %.

Colour coding is red: glucose cultivation, blue: glucose and malate cultivation, green: glucose and fumarate and yellow: glucose and citrate. Colour intensity increases with ongoing cultivation time.

Amino acid pools

Altogether, our results show that differences in the intracellular metabolite pool under the growth conditions investigated are marginal, especially compared to those observed in the exo-metabolome. This confirms the assumption that *B. subtilis* is able to maintain a steady intracellular metabolite pool independently of the available carbon source. To support this hypothesis, the composition of the free amino acids was compared between all four growth conditions. The mean values of amino acid concentrations in exponential (four time points) and in stationary phase (two time points) were calculated and the proportion of each amino acid was calculated. Arginine, asparagine and tryptophan were not taken into consideration. Arginine is not accessible in GC/MS measurements due to decomposition processes during derivatization or analysis. Asparagine and tryptophan could not be detected because their concentrations were below the limit of detection.

The composition of the free amino acids was similar between the four growth conditions (Figure 4 and Supplementary Figure 1). In all cases, glutamate was by far the most abundant intracellular amino acid, present in concentrations about 200-300 nmol/mg CDW, as shown before[19]. Moreover, the amino acid proportions did not vary considerable between exponential and stationary growth phase. The only clear differences noted were lower proportions of glutamine and a higher proportion of aspartate for cells of the stationary phase compared to those of the exponential phase. These data confirm the hypothesis that *B. subtilis* is able to maintain a stable intracellular metabolite pool.

Molecular BioSystems Accepted Manuscript

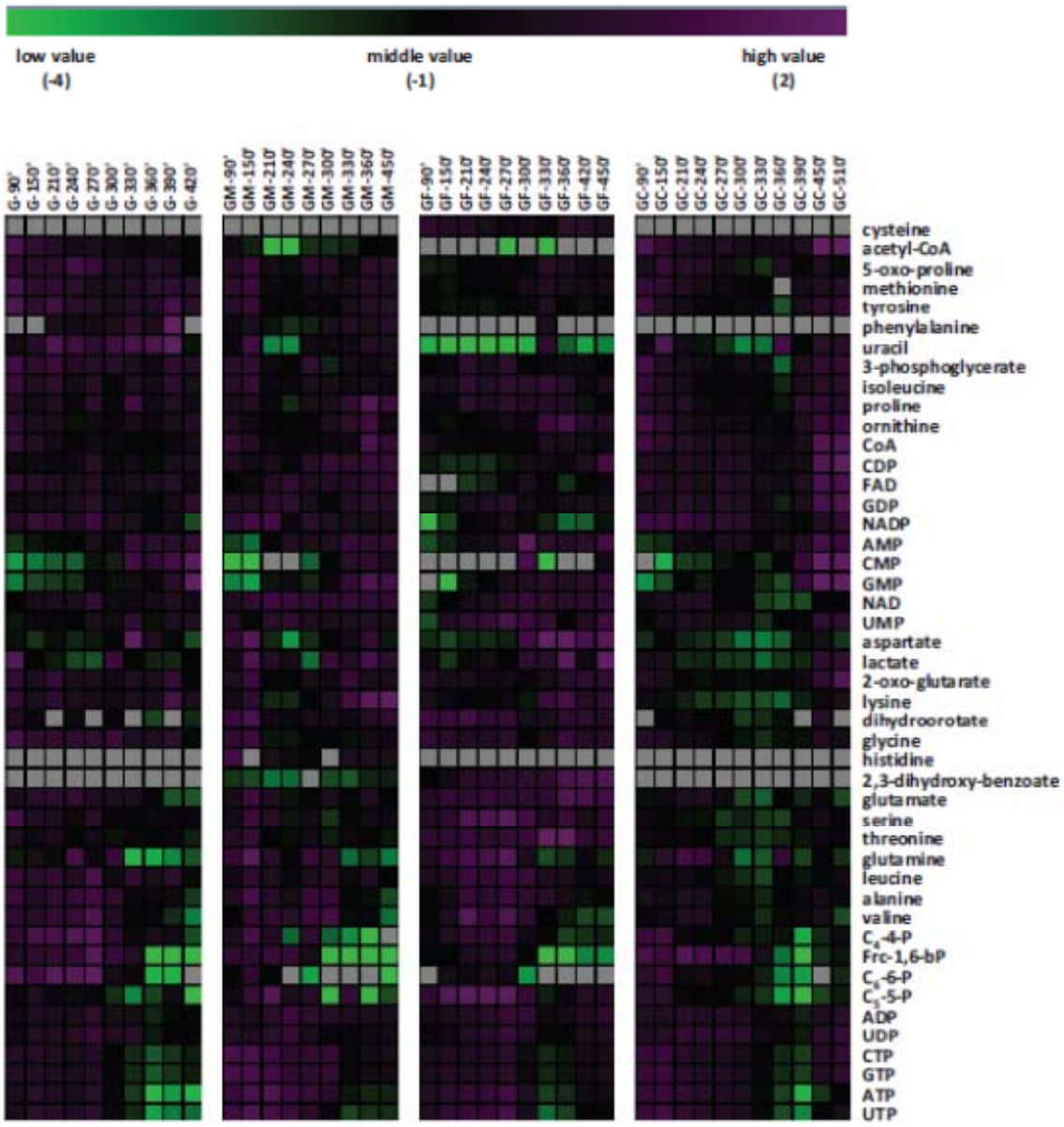

Figure 4: Heatmap visualization for all quantified intracellular metabolites. Left: only glucose (G) followed by glucose and malate (GM) and: glucose and fumarate (GF) and right: glucose and citrate (GC). The heatmap represents changes in metabolite concentration [nmol/ mg CDW] as $\log_2$ ratio of the mean metabolite concentration at each time point referred to the average concentration [nmol/ mg CDW] of respective metabolite at all time points and under all conditions. Purple: lower concentration limit and green: upper concentration limit. C_6-6-P, C_5-5-P and C_4-4-P: a sugar-phosphate containing of six, five or four carbon atoms, respectively.

Molecular BioSystems Accepted Manuscript

During growth with glucose and malate, an extracellular accumulation of valine and leucine was observed. Hence, higher intracellular concentrations of the latter metabolites might be expected. On the other hand, maintenance of intracellular metabolite equilibrium might require their secretion. Isoleucine, leucine and valine were present intracellularly in concentrations of up to 1 nmol/mg CDW, 1-2 nmol/mg CDW, and max. 10 nmol/mg CDW, respectively and their concentrations were comparable in all four growth conditions (Figure 4 and Supplementary Figure 1). Thus, besides regulatory events influencing mRNA, protein or flux level, different metabolite secretion profiles might enable *B. subtilis* to maintain this intracellular metabolite equilibrium.

Glycolysis intermediates

While the overall metabolite pool was very similar between all conditions and remained almost steady between exponential and stationary growth phase, specific, growth-phase dependent metabolic changes were uncovered.

Since glycolysis is mainly active as long as suitable carbon sources such as glucose are available, the possibility that glycolysis intermediates are present at higher levels during exponential growth compared to stationary phase was tested. A concentration decrease in stationary growth phase was mainly observed for fructose-1,6-bis-phosphate (Figure 5). The other glycolysis intermediates exhibited steady concentrations during growth and phosphoenolpyruvate and 1,3-bisphosphoglycerate could not be detected. This decrease in the concentration of fructose-1,6-bis-phosphate is consistent with the role of phosphofructokinase (Pfk) in catalysis of a key regulatory step in the glycolysis[28, 29].

Molecular BioSystems Accepted Manuscript

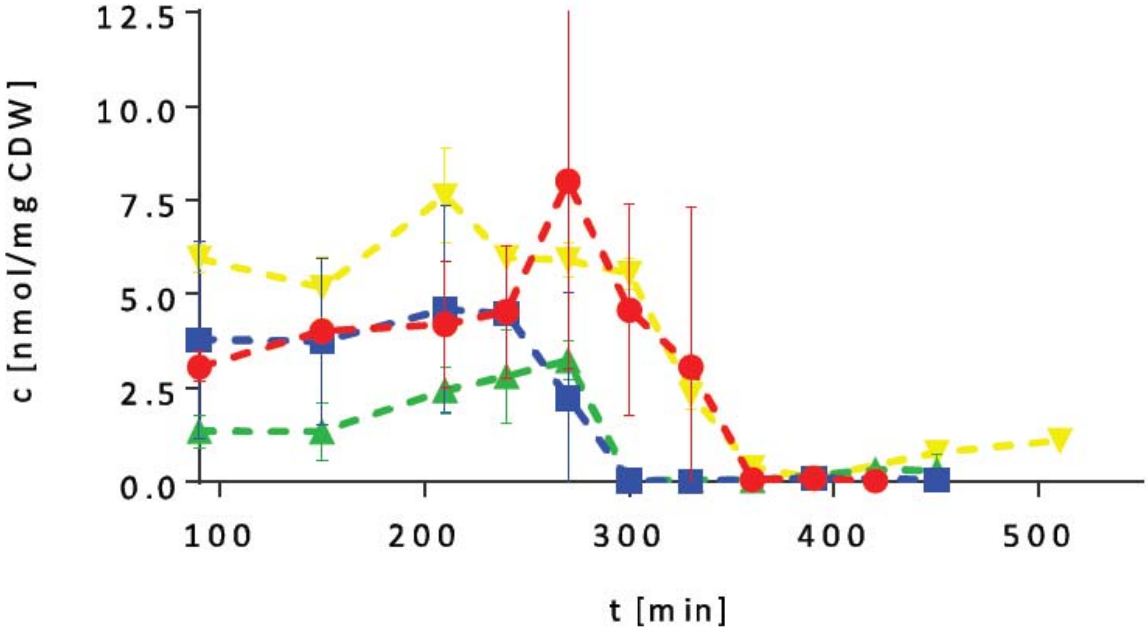

Figure 5: Fructose-1,6-bis-phosphate concentration.

The concentration of fructose-1,6-bis-phosphate [nmol/ mg CDW] is plotted against the time of cultivation in [min] for red: only glucose, blue: glucose and malate, green: glucose and fumarate and yellow: glucose and citrate.

Moreover fructose-1,6-bis-phosphate, beside glucose-6-phosphate functions as a fine-tuning effector during carbon catabolite repression[15]. High concentrations of ATP and fructose-1,6-bis-phosphate indicate strong glycolytic activity in the presence of the preferred carbon source.

In *B. subtilis,* CCR is mediated by the histidine containing protein HPr of the phosphotransferase system (PTS), the bifunctional HPr kinase/phosphorylase (HPrK) and the catabolite control protein A (CcpA) which is a pleiotropic transcription factor[30]. HPr is phosphorylated at Ser46 by HPrK if the intracellular concentration of ATP is high. The HPrK activity is enhanced by high concentrations of fructose-1,6-bis-phosphate. Moreover, the interaction between HPr-Ser46-P and CcpA or/and the affinity of the CcpA-HPr-P complex to the DNA is improved by glucose-6-phosphate and fructose-1,6-bis-phosphate[15, 31]. Our time resolved metabolome analysis support this model. As long as glucose was available and the glycolysis was active fructose-1,6-bis-phosphate levels were high preventing

Molecular BioSystems Accepted Manuscript

expression of CcpA repressed genes. When glucose was exhausted, fructose-1,6-bis-phosphate levels dropped permitting formerly CcpA-repressed genes to scavenge alternative carbon sources.

Nucleoside triphosphates (NTPs) and Energy charge

ATP is used in cells as cofactor for energy transfer. During nutrient excess the intracellular ATP level is known to be high, which was also observed in this study for exponentially growing cells (Figure 6). Highest ATP concentrations were monitored for cells grown on glucose and malate. Since glucose and malate consumption occur in parallel, higher ATP concentrations were accomplished under this condition. For cells grown on glucose and fumarate, ATP concentration increased simultaneously with the initiation of fumarate utilization. The lowest ATP concentration during exponential growth was monitored for cells grown on only glucose. Under all conditions investigated, the ATP concentration decreased markedly when glucose was exhausted and cells entered the stationary growth phase (Figure 6). For cells grown on glucose and fumarate and for growth on glucose and citrate, the ATP concentration increased slightly after glucose was utilized and cells alternatively used the second carbon source available. Similar concentration trends were observed for ADP. In the exponential growth phase ADP concentration increased slightly during growth on glucose and malate and glucose and fumarate reaching a peak when glucose was consumed and then declined during entry into stationary phase. ADP levels then increased again on glucose and fumarate and glucose and citrate, probably because these alternative carbon sources were used. For cells grown on glucose or glucose and malate such an increase in ADP beyond 350 min was not observed because both glucose and malate were consumed. AMP increased slightly and continuously when bacilli entered the stationary phase under all cultivation conditions (Figure 6).

Molecular BioSystems Accepted Manuscript

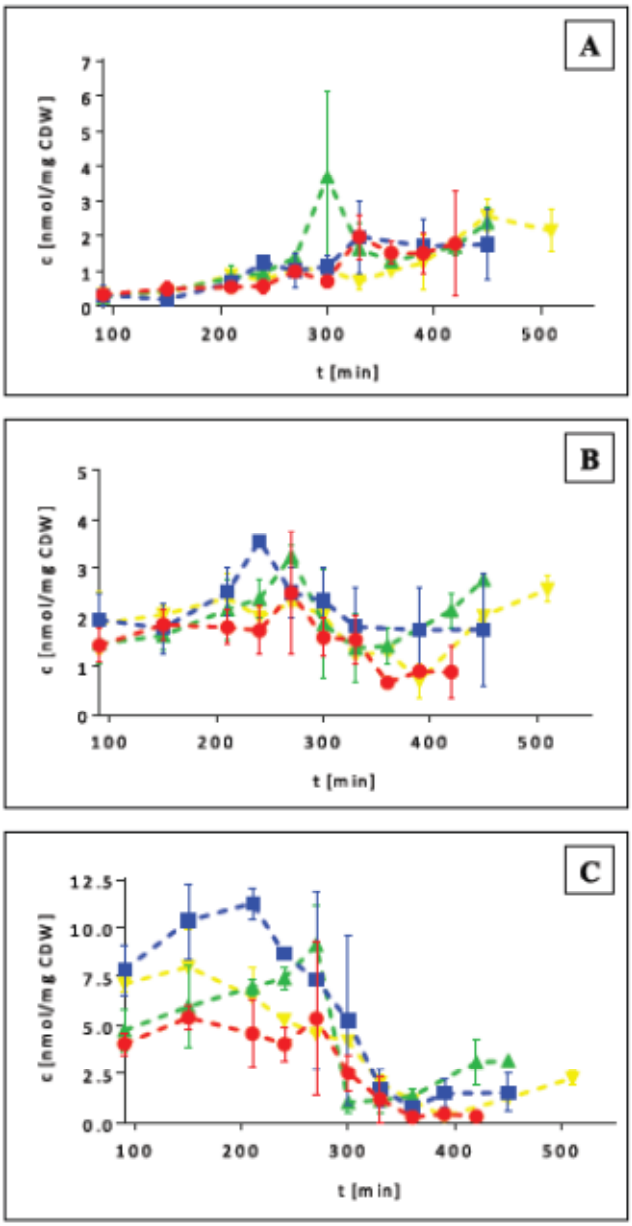

344

345 ***Figure 6:*** Adenosine phosphates.

346 The concentration of A) AMP, B) ADP and C) ATP in [nmol/ mg CDW] is plotted against the time of
347 cultivation in [min] for red: only glucose, blue: glucose and malate, green: glucose and fumarate and
348 yellow: glucose and citrate.

349

350 The concentration of AMP, ADP and ATP can be used to calculate the adenylate energy charge (EC)
351 of cells. The EC is defined as (EC = [ATP] + ½ [ADP]) / ([AMP] + [ADP] + [ATP]) and reflects the energy
352 status of a cell. Under all conditions, the EC was over 0.8 during exponential growth. When cells
353 entered stationary phase due to the consumption of one or both carbon sources, the EC decreased

Molecular BioSystems Accepted Manuscript

(Figure 7). Only minor differences in the EC trend were observed between the four conditions investigated. When cells entered the stationary phase the drop in the EC was strongest during cultivation on only glucose and glucose and fumarate. If cells were grown on glucose and citrate the energy charge decreased slightly slower. A substantial increase in the EC was detectable for growth on glucose and fumarate, which was less pronounced for glucose and citrate and in both cases likely triggered by the utilization of the second carbon source (Figure 7). This increase in the EC was caused by the slight increases of ADP and ATP, observed under these growth conditions (Figure 6).

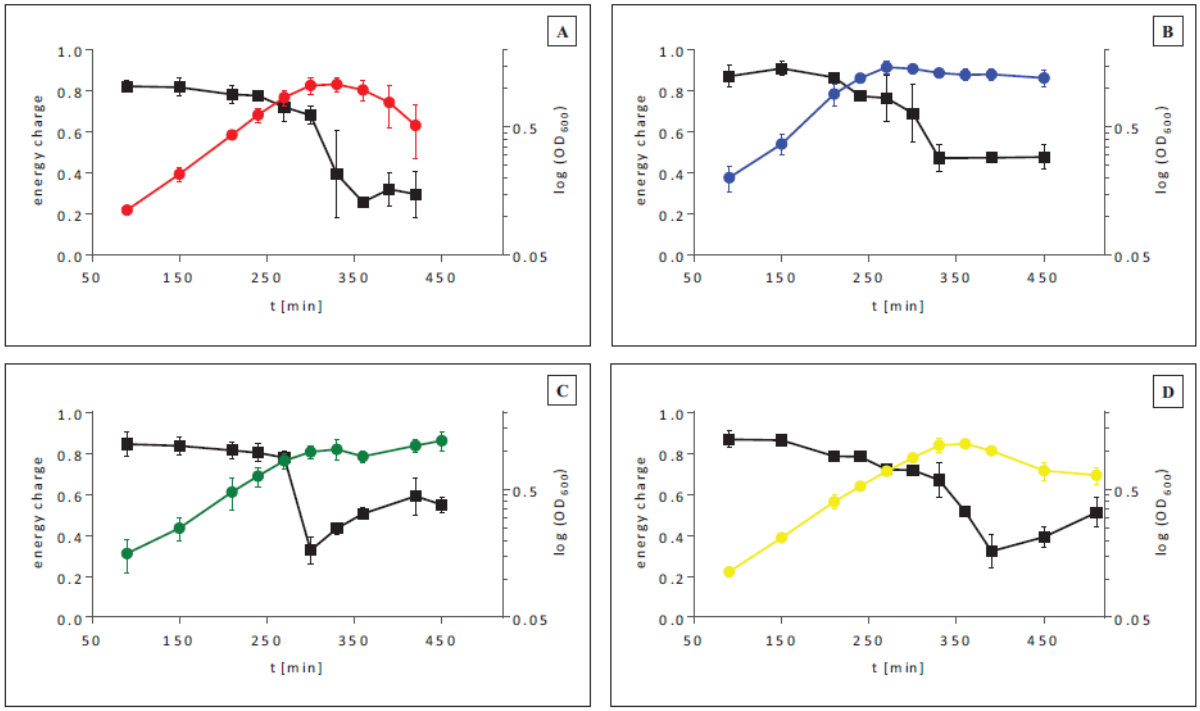

***Figure 7**:* Growth curves and energy charge trends for A) only glucose, B) glucose and malate, C) glucose and fumarate and D) glucose and citrate. Black lines illustrate the energy charge trend and the coloured lines the growth curve.

The levels of the other three nucleoside triphosphates (UTP, CTP and GTP) displayed a pattern comparable to ATP and decreased significantly during entry into stationary, because carbon/energy source supply was limiting (Figure 4 and Supplementary Figure 2). With glucose and fumarate and

Molecular BioSystems Accepted Manuscript

glucose and citrate as combined carbon sources UTP, CTP (Figure 4) and particularly GTP levels (Figure 4 and Supplementary Figure 2) similar to ATP were recovered, when *B. subtilis* initiated utilization of fumarate or citrate. GMP and GDP concentration increased similarly under these conditions (Supplementary Figure 2).

Activation of the alternative RNA polymerase sigma factor σ^B during entry into stationary phase.

The alternative RNA polymerase sigma factor σ^B controls the large general stress regulon of *B. subtilis* which is activated by a wide range of environmental stimuli including nutrient limitation[6, 32]. Changes in the ATP level have been postulated to be crucial for the σ^B activation of *B. subtilis* during energy limitation[33-37] early on, but definite proof is still lacking. Therefore, we also wanted to investigate the impact of the different carbon source combinations on the ability of *B. subtilis* to mount the general stress response during entry into the stationary phase. σ^B activity was monitored with the aid of an established *ctc::lacZ* reporter gene fusion[38]. Contrary to our assumption, a strong activation of σ^B was only recorded when *B. subtilis* grown on either glucose or glucose and malate entered the stationary phase (Figure 8). For cells grown on glucose and fumarate or glucose and citrate, significant activation of the σ^B-dependent *ctc::lacZ* fusion was not observed, although the entry into stationary phase causes a concomitant drop in ATP concentration. A closer inspection of the ATP-levels and EC then provided a potential clue for the failure of *B. subtilis* to mount the σ^B-dependent general stress response during entry into stationary phase in glucose and fumarate or glucose and citrate medium.

Molecular BioSystems Accepted Manuscript

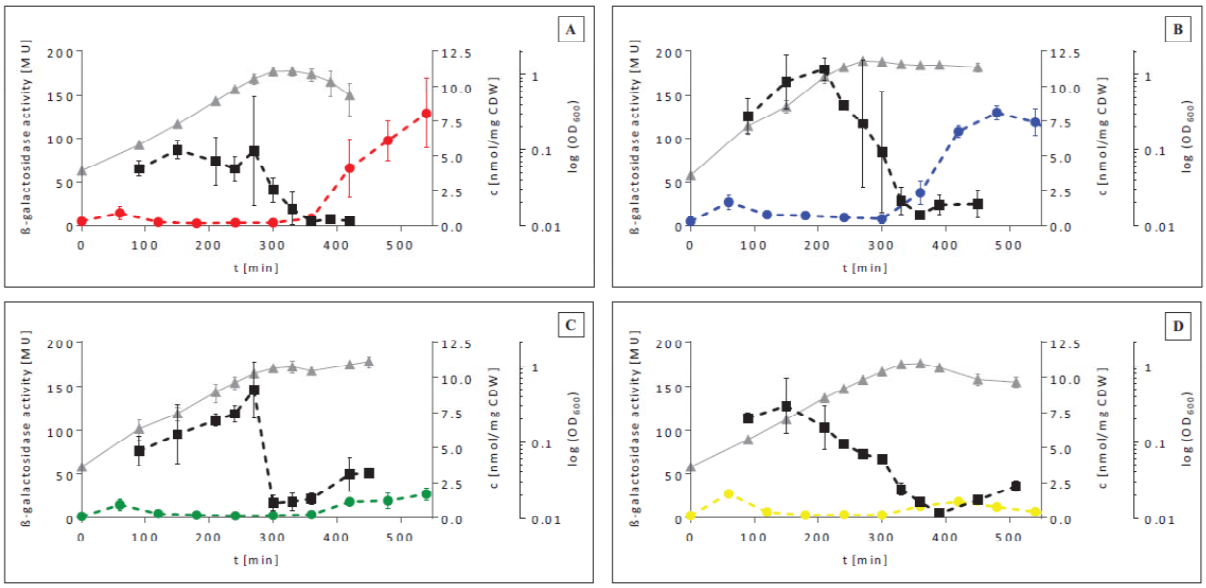

***Figure 8**:* Growth behaviour, σ^B activity and ATP concentration.

Bacterial growth was monitored by optical density measurement (OD) at 600nm. Represented as grey lines is the $\log_{10}$ value of the OD. σ^B activity was monitored with the aid of an *ctc:lacZ*-fusion and is presented in Miller units [MU] as coloured lines. The ATP concentrations in [nmol/ mg CDW] are plotted against the time of cultivation in [min] as black lines. A) only glucose, B) glucose and malate, C): glucose and fumarate and D) glucose and citrate.

Even if under both conditions a sharp decline in the ATP-level was observed during entry into stationary phase, this low level ATP was not maintained but ATP-levels started to recover when fumarate or citrate were then subsequently used as carbon sources (Figure 6). This utilization of the two alternative carbon sources was also reflected in the EC which did not decrease to the same low level as during cultivation with glucose only and started to recover shortly after the minimum level was reached (Figure 7). The pattern was different for growth on glucose and malate. Both were co-metabolized straight from the beginning, permitting high levels of ATP and a high EC, which then dramatically declined when both carbon sources were exhausted (Figures 6 and 7). Although the minimal levels reached were not as low as during growth on glucose alone, they remained permanently low, apparently allowing full activation of the σ^B-dependent general stress response.

Molecular BioSystems Accepted Manuscript

For GTP, which has also been described to be involved in σ^B activation[36], similar trends as for ATP, i.e. sharp drops and constant low levels on glucose and glucose and malate but recovering pools on glucose and fumarate and glucose and citrate were observed (Supplementary Figure 2). Thus, the data generated in this metabolome study support a role of ATP and GTP in the control of the activity of σ^B. However, since the observations are based on associations only, we cannot proof if ATP or GTP pools directly control activity of σ^B or whether other low molecular weight effectors that follow the concentration patterns of ATP/GTP are the direct mediators. However, the absence of σ^B activation during entry into stationary phase in glucose and fumarate and glucose and citrate medium indicates that ATP/GTP concentrations have to remain low and must not recover to sustain activation of σ^B.

Conclusion:

In this study the influence of different carbon source combinations on the intracellular and extracellular metabolome of *B. subtilis* was determined along the growth curve.

A global perspective of the sum of all quantitative metabolite data was gained by principal component analysis. This PCA confirmed main differences between the four growth conditions in the exo-metabolome, which is illustrated by the clear cluster separation of the extracellular metabolite samples according to carbon source supply and the growth phase (Figure 3A). A comparable cluster separation was not observed for the intracellular metabolite samples, indicating less carbon source and growth dependent differences in the intracellular metabolome (Figure 3b). Regulatory systems on the transcriptome, proteome and flux level appear to be able to sustain a stable intracellular metabolite pool. Furthermore, our study implies that possibly this intracellular metabolite equilibrium is also maintained via different metabolite secretion profiles.

In the exo-metabolome, the strongest accumulation of overflow metabolites was observed during growth on glucose and malate, which were co-metabolized. Surplus metabolic capacity in glucose and malate grown cells, triggered extensive secretion of metabolites, probably caused by high rate of glycolysis, and the resulting high energy status of the cell.

Molecular BioSystems Accepted Manuscript

Several studies have been carried out analysing the central carbon metabolism and the overflow metabolism of *B. subtilis.* Recently, an extensive work of the "Global network reorganization during dynamic adaptations of *B. subtilis* metabolism" was published[19]. Nevertheless, still comparably little is known about "uncommon overflow metabolism". This is the first approach that uncovers cultivation condition dependent differences in the secretion of leucine and valine and some intermediates of the BCAA and BCFA. A secretion of these metabolites was mainly observed when glucose and malate were used as carbon sources.

Furthermore, to our knowledge, this is the first time that the energy charge trend during growth of *B. subtilis* is described. Contrary to the overall metabolite pool, *B. subtilis* is not able to maintain a steady EC when cells enter stationary phase.

The correlation of metabolite levels and σ^B activity support the established model of critical roles of ATP and GTP in regulation of σ^B activity and provide hints that ATP/GTP levels or those of further metabolites have to be maintained to permit strong, σ^B-mediated expression of the general stress regulon of *B. subtilis.*

Thus, these time-resolved metabolome data will provide a valuable resource for the reconstruction of a comprehensive metabolic network of *B. subtilis*.

Material and Methods:

Cultivation

B. subtilis (168trp$^+$ with *ctc::lacZ* and *gsib::gfp* reporter gen fusions[39, 40]) was cultivated in chemical defined M9 medium containing 0.1% glucose with additional 0.1% malate, fumarate or citrate as indicated. LB plates of *B. subtilis* were prepared from frozen stocks (-80 °C, in 15% (v/v) glycerol) and incubated at 37 °C for 24 h. For the pre-culture, 5 ml LB medium including 1µg/ml erythromycin and 5 µg/ml chloramphenicol antibiotics were inoculated with colonies from the abovementioned plate. The cells were incubated for 14 h at 37 °C and 240 rpm. Before inoculation of the main culture to an OD_{600nm} of 0.05, the overnight culture was tested to ensure it was in exponential growth phase

Molecular BioSystems Accepted Manuscript

(OD_{600nm} = 0.4-0.8). The main culture was incubated in shake flasks under aerobic conditions at 37 °C and steady shaking at 300 rpm.

β-Galactosidase-Assay

Sigma-B activation was measured as Miller units of the β-galactosidase as described previously[34, 40]. 200 µl o-nitrophenyl-β-D-galactopyranosid (4 mg/ ml Z-buffer) was used as enzyme subtrate.

Extracellular metabolite sampling, measurement by ^{1}H-NMR and data analysis

Two ml cell culture was rapidly sterile syringe filtrated (ø pore 0.45 µm, Filtropur S®, Sarstedt) and the sample was stored at -20°C prior to measurement. For analysis 400 µl of the extracellular sample was buffered to pH 7.0 by addition of 200 µl of a sodium hydrogen phosphate buffer (0.2 M [pH 7.0], including 1 mM TSP) made up with 50 % D_2O to provide a nuclear magnetic resonance (NMR)-lock signal. Data analysis was implemented by AMIX® (Bruker Biospin)[41].

Intracellular metabolite sampling

Samples for intracellular metabolome analysis were obtained by a fast vacuum dependent filtration using 0.45 µm filters (S-pak®, Millipore)[42] as described previously[43]. For this purpose 10-20 OD units of the main culture were poured into a 50 mL falcon tube and cooled with liquid nitrogen for 10 sec (sample temperature after cooling 9±2°C). For metabolite extraction and cell disruption, samples were thawed on ice (≤ 6°C) and internal standards were added (20 nmol ribitol and norvaline for GC-MS and 2.5 nmol camphor sulfonic acid for LC-MS analysis). Afterwards samples were vortexed and shaken 10 times alternately and centrifuged for 5 min at 4 °C and 13000 rpm. The supernatant was transferred to a new falcon tube, while the pellet was once more extracted using cold water. The supernatants were combined and restocked with double-distilled water to a final organic solution concentration of 10 % and stored at -80 °C prior to lyophilization.

Molecular BioSystems Accepted Manuscript

IP-LC-MS: Intracellular metabolite measurement and analysis

Ion pairing-LC-MS measurement (IP-LC-MS) was performed using an Agilent HPLC System (1100; Agilent Technologies, USA) coupled to a Bruker micrOTOF mass spectrometer (Bruker Daltonics, Bremen, Germany). The Agilent HPLC System was equipped with a quaternary pump, an online degasser, and an autosampler.

Completely lyophilized samples were dissolved in 100 µl double-distilled water and centrifuged for 2 min (13.000 rpm, 4 °C). The supernatants were transferred into glass vials with micro inserts for small volume injections.

Chromatographic separation was performed using a RP-C_{18} column (3.5 µm, 150x4.6 mm) with a C_{18} pre-column. The mobile phase composition was: A: 5% methanol and 95% water, containing 10 mM tributylamine as ion-pairing reagent and 15 mM acetic acid for pH adjustment to pH 4.9 and B: 100% methanol. A Bruker micrOTOF (Bruker Daltonik, Bremen, Germany) mass spectrometer was operating in ESI negative mode using a mass range from 50 to 3000 m/z.

Metabolite signal integration was done by QuantAnalysis® (Bruker Daltonik, Bremen, Germany). Peak areas of extracted ions were normalized to the internal standard area of camphorsulfonic acid. For determination of the calibration equation, different concentrations of pure standards were measured and analyzed in the same manner. Calibration was done via a polynomial regression of degree 2 and a 1/x weighting by GraphPad Prism®. The computed metabolite concentrations were further normalized to the sample volume and related to the respective cell dry weight.

Intracellular metabolite measurement GC-MS

GC-MS (EI quadrupol) analysis was performed using an Agilent DB-5ms column. Completely lyophilized samples were derivatized for 90 min at 37 °C with MeOX and 30 min at 37 °C with MSTFA. After centrifugation for 2 min at room temperature the supernatant was transferred into GC-Vials prior to measurement as described previously[44].

Metabolite signal integration was done by GaVin[45] and the peak areas of extracted ions were normalized to the area of the internal standard ribitol. For determination of the calibration equation,

Molecular BioSystems Accepted Manuscript

different concentrations of pure standard compounds were measured and analyzed in the same manner. Calibration was done via a polynomial regression of degree 2 and a 1/x weighting by GraphPad Prism®. The computed metabolite concentrations were further normalized to the sample volume and related to the respective cell dry weight.

Significance

Significance tests were performed by Microsoft Excel®. The two-sided homoscedastic T-test was used to calculate p-values. Metabolite concentrations were indicated to be significantly different if the calculated p-value was lower than 0.05. For exact p-values see supplementary table 3.

Acknowledgement:

We thank Jana Priebe and Sylvia Härtel for technical assistance and Henrik Strahl von Schulten for helpful discussion. Furthermore we thank Baltic Analytics for laboratory infrastructure. This work was supported by the Bundesministerium für Bildung und Forschung (BMBF, BACELL-SysMO1&2 031397A and 0315784A).

References:

1. Schallmey M, Singh A, Ward OP. *Canadian Journal of Microbiology* 2004, **50**, 1-17
2. Dooley DC, Hadden CT, Nester EW. *J Bacteriol* 1971, **108**, 668-79
3. Stein T. *Mol Microbiol* 2005, **56**, 845-57
4. Fickers P. *American Journal of Biochemistry and Biotechnology* **8**, 40-46
5. Otto A, Bernhardt J, Meyer H, Schaffer M, Herbst FA, Siebourg J, Mader U, Lalk M, Hecker M, Becher D. *Nat Commun* 2010, **1**, 1-9
6. Hecker M, Volker U. *Advances in microbial physiology* 2001, **44**, 35-91
7. Budde I, Steil L, Scharf C, Volker U, Bremer E. *Microbiology* 2006, **152**, 831-53
8. Dauner M, Storni T, Sauer U. *Journal of Bacteriology* 2001, **183**, 7308-17
9. Hecker M, Schumann W, Volker U. *Mol Microbiol* 1996, **19**, 417-28
10. Hahne H, Mader U, Otto A, Bonn F, Steil L, Bremer E, Hecker M, Becher D. *J Bacteriol* **192**, 870-82
11. Petersohn A, Bernhardt J, Gerth U, Hoper D, Koburger T, Volker U, Hecker M. *J Bacteriol* 1999, **181**, 5718-24
12. Liebeke M, Brozel VS, Hecker M, Lalk M. *Appl Microbiol Biotechnol* 2009, **83**, 161-73
13. Ye BC, Zhang Y, Yu H, Yu WB, Liu BH, Yin BC, Yin CY, Li YY, Chu J, Zhang SL. *PloS one* 2009, **4**, e7073
14. van der Werf MJ, Overkamp KM, Muilwijk B, Koek MM, van der Werff-van der Vat BJC, Jellema RH, Coulier L, Hankemeier T. *Mol Biosyst* 2008, **4**, 315-27

Molecular BioSystems Accepted Manuscript

15. Görke B, Stülke J. *Nat Rev Microbiol* 2008, **6**, 613-24
16. Meyer FM, Jules M, Mehne FM, Le Coq D, Landmann JJ, Gorke B, Aymerich S, Stulke J. *J Bacteriol* 2011, **193**, 6939-49
17. Singh KD, Schmalisch MH, Stulke J, Gorke B. *J Bacteriol* 2008, **190**, 7275-84
18. Kleijn RJ, Buescher JM, Le Chat L, Jules M, Aymerich S, Sauer U. *J Biol Chem* 2010, **285**, 1587-96
19. Buescher JM, Liebermeister W, Jules M, Uhr M, Muntel J, Botella E, Hessling B, Kleijn RJ, Le Chat L, Lecointe F, Mader U, Nicolas P, Piersma S, Rugheimer F, Becher D, Bessieres P, Bidnenko E, Denham EL, Dervyn E, Devine KM, Doherty G, Drulhe S, Felicori L, Fogg MJ, Goelzer A, Hansen A, Harwood CR, Hecker M, Hubner S, Hultschig C, Jarmer H, Klipp E, Leduc A, Lewis P, Molina F, Noirot P, Peres S, Pigeonneau N, Pohl S, Rasmussen S, Rinn B, Schaffer M, Schnidder J, Schwikowski B, Van Dijl JM, Veiga P, Walsh S, Wilkinson AJ, Stelling J, Aymerich S, Sauer U. *Science* 2012, **335**, 1099-103
20. Lerondel G, Doan T, Zamboni N, Sauer U, Aymerich S. *J Bacteriol* 2006, **188**, 4727-36
21. Doan T, Servant P, Tojo S, Yamaguchi H, Lerondel G, Yoshida K, Fujita Y, Aymerich S. *Microbiology* 2003, **149**, 2331-43
22. Schilling O, Frick O, Herzberg C, Ehrenreich A, Heinzle E, Wittmann C, Stulke J. *Appl Environ Microbiol* 2007, **73**, 499-507
23. Grundy FJ, Waters DA, Takova TY, Henkin TM. *Mol Microbiol* 1993, **10**, 259-71
24. Huang M, Oppermann-Sanio FB, Steinbuchel A. *J Bacteriol* 1999, **181**, 3837-41
25. Grundy FJ, Turinsky AJ, Henkin TM. *Journal of Bacteriology* 1994, **176**, 4527-33
26. Ali NO, Bignon J, Rapoport G, Debarbouille M. *J Bacteriol* 2001, **183**, 2497-504
27. Shulman A, Zalyapin E, Vyazmensky M, Yifrach O, Barak Z, Chipman DM. *Biochemistry-Us* 2008, **47**, 11783-92
28. Garland PB, Randle PJ, Newsholme EA. *Nature* 1963, **200**, 169-70
29. Dobson GP, Yamamoto E, Hochachka PW. *The American journal of physiology* 1986, **250**, R71-6
30. Fujita Y. *Bioscience, biotechnology, and biochemistry* 2009, **73**, 245-59
31. Schumacher MA, Seidel G, Hillen W, Brennan RG. *J Mol Biol* 2007, **368**, 1042-50
32. Wise AA, Price CW. *J Bacteriol* 1995, **177**, 123-33
33. Alper S, Dufour A, Garsin DA, Duncan L, Losick R. *J Mol Biol* 1996, **260**, 165-77
34. Voelker U, Voelker A, Maul B, Hecker M, Dufour A, Haldenwang WG. *J Bacteriol* 1995, **177**, 3771-80
35. Dufour A, Haldenwang WG. *Journal of Bacteriology* 1994, **176**, 1813-20
36. Zhang S, Haldenwang WG. *J Bacteriol* 2005, **187**, 7554-60
37. Maul B, Volker U, Riethdorf S, Engelmann S, Hecker M. *Mol Gen Genet* 1995, **248**, 114-20
38. Benson AK, Haldenwang WG. *J Bacteriol* 1993, **175**, 1929-35
39. Botella E, Fogg M, Jules M, Piersma S, Doherty G, Hansen A, Denham EL, Le Chat L, Veiga P, Bailey K, Lewis PJ, van Dijl JM, Aymerich S, Wilkinson AJ, Devine KM. *Microbiology* 2010, **156**, 1600-8
40. Liebal UW, Sappa PK, Millat T, Steil L, Homuth G, Volker U, Wolkenhauer O. *Mol Biosyst* 2012, **8**, 1806-14
41. Liebeke M, Dorries K, Zuhlke D, Bernhardt J, Fuchs S, Pane-Farre J, Engelmann S, Volker U, Bode R, Dandekar T, Lindequist U, Hecker M, Lalk M. *Mol Biosyst* 2011, **7**, 1241-53
42. Meyer H, Liebeke M, Lalk M. *Anal Biochem* 2010, **401**, 250-9
43. Meyer H, Weidmann H, Lalk M. *Microb Cell Fact* 2013, **12**, 69
44. Liebeke M, Pother DC, van Duy N, Albrecht D, Becher D, Hochgrafe F, Lalk M, Hecker M, Antelmann H. *Mol Microbiol* 2008, **69**, 1513-29
45. Behrends V, Tredwell GD, Bundy JG. *Anal Biochem* 2011, **415**, 206-8

Molecular BioSystems Accepted Manuscript